Proc. Natl. Acad. Sci. USA
Vol. 89, pp. 10021–10025, November 1992
Plant Biology

Photosynthetic membrane topography: Quantitative *in situ* localization of photosystems I and II

(immunolabeling/*Porphyridium*/phycobilisome)

LASZLO MUSTARDY*, FRANCIS X. CUNNINGHAM, JR., AND ELISABETH GANTT†

Department of Botany and Maryland Agricultural Experiment Station, University of Maryland, College Park, MD 20742

Communicated by Jack Myers, July 14, 1992 (received for review March 17, 1992)

ABSTRACT **An immunolabeling approach was developed for quantitative *in situ* labeling of photosystems I and II (PSI and PSII). Photosynthetic membranes from the phycobilisome-containing red alga *Porphyridium cruentum* were isolated from cells in which different photosystem compositions were predetermined by growing cells in green light (GL) or red light (RL). Based on phycobilisome densities per membrane area of 390 per μm^2 (GL) and 450 per μm^2 (RL) and the PSI reaction center (P_{700}) and PSII reaction center (Q_A) content, the photosystem densities per μm^2 of membrane were calculated to be 2520 PSI in GL and 1580 in RL and 630 PSII in GL and 1890 in RL. PSI was detected in the membranes with 10-nm Au particles conjugated to affinity-purified anti-PSI, and PSII was detected with 15-nm Au particles conjugated to anti-PSII. Distribution of Au particles appeared relatively uniform, and the degree of labeling was consistent with the calculated photosystem densities. However, the absolute numbers of Au-labeled sites were lower than would be obtained if all reaction center monomers were labeled. Specific labeling of PSI was 25% in GL and RL membranes, and PSII labeling was 33% in GL but only 17% in RL membranes. An IgG–Au particle is larger than a monomer of either photosystem and could shield several closely packed photosystems. We suggest that clustering of photosystems exists and that the cluster size of PSI is the same in GL and RL cells, but the PSII cluster size is 2 times greater in RL than in GL cells. Such variations may reflect changes in functional domains whereby increased clustering can maximize the cooperativity between the photosystems, resulting in enhancement of the quantum yield.**

Photosynthesis is a biological process whose efficiency depends on the coordinated interaction of several participating protein complexes that reside in the photosynthetic membrane. Our understanding of the photosynthetic membrane structure is largely derived from studies on fractionated membranes and from conventional electron microscopy (1, 2), and our knowledge of the spatial and functional interaction between principal membrane complexes is quite limited. Such information is directly relevant to excitation energy transfer as well as to the diffusion of mobile electron carriers (3, 4) in photosynthetic membranes of oxygen-evolving plants. Major integral protein complexes include ATP synthase, cytochrome b_6/f, photosystem I (PSI), and photosystem II (PSII) and LHCII in green plants. In phycobilisome (PBsome)-containing organisms—namely, red algae and cyanobacteria—the LHCII complex appears to be absent and PBsomes on the stromal surface serve as the principal light-harvesting antennae (5).

In PBsome-containing organisms it is generally assumed that the arrangement of the photosystems in the thylakoid is predictable from the PSII/phycobiliprotein ratio (6, 7) and that the PBsome distribution on the stromal surface is indicative of the PSII location (8, 9). Since PBsomes with PSII activity have been isolated, a direct functional association exists *in vivo* (10), although a direct interaction between PBsomes and PSI cannot be ruled out. The following questions are being addressed here: (*i*) how many PSI and PSII centers exist per unit of surface area, (*ii*) is the distribution of PSI and PSII uniform throughout the membrane, (*iii*) are the photosystems present as monomers or as clusters, and (*iv*) if they are clustered, does the cluster size change under different growth conditions?

By conventional immunocytochemical methods, the subcellular distribution of proteins in plants is well established, including specific localization of a number of chloroplast components in land plants and algae (1, 11, 12). We have shown that this approach can be used to provide a quantitative measure of the relative amounts of PSI and PSII in *Porphyridium cruentum* (13, 14). However, since antigenic sites are accessible only on exposed surfaces of embedded sections, the absolute number of particular components is greatly underestimated, and spatial distances between individual complexes are difficult to ascertain.

To ascertain the spatial relationships of PSI and PSII requires intact membranes and a means of identifying the photosystems. By freeze-fracture, 10-nm particles exposed on the exoplasmic fracture face are regarded as representing PSII centers. The isolation of PSII particles and their visualization in lipid vesicles support this attribution (15). Also, there is good evidence that some 10- to 13-nm particles on the protoplasmic fracture face represent PSI (2), but one cannot identify individual particles as photosystems. Since PSI and PSII particles are not identifiable in the same fracture-face, meaningful spatial correlations are difficult if not impossible at present. By using Au-conjugated antibodies, Hinshaw and Miller (16) labeled a PSII antenna complex in occluded surfaces in frozen membranes. Potential movement of proteins is unlikely, but a major limitation is the small size of exposed membrane surfaces available, thus making quantitative assessments difficult.

We devised an approach for *in situ* labeling of PSI and PSII in thylakoid membranes of the red alga *P. cruentum*. The PSI was localized with an antiserum specific for two chlorophyll-binding proteins (presumed gene products of *psaA* and *psaB*) (13). For PSII, an antiserum to a proximal core antenna polypeptide (CP47), the presumed gene product of *psbB*, was used (13). In this report, we use the designations of PSI and PSII, respectively, since the immunologically recognized polypeptides are representative of the reaction center cores. Large thylakoid membrane sheets were isolated from cells

The publication costs of this article were defrayed in part by page charge payment. This article must therefore be hereby marked "*advertisement*" in accordance with 18 U.S.C. §1734 solely to indicate this fact.

Abbreviations: PSI, photosystem I; PSII, photosystem II; PBsome, phycobilisome; GL, green light; RL, red light.

*Present address: Institute of Plant Physiology, Biological Research Center, Hungarian Academy of Sciences, P.O. Box 521, Szeged, Hungary H6701.

†To whom reprint requests should be addressed.

grown under two different light regimes which result in very different and well-defined stoichiometries of PSI and PSII (17). Membrane isolation involved mild cell breakage and handling at a temperature (4°C) that is assumed to be below the lipid-phase transition point of the membranes, since the cell-growth temperature was ≈18°C. In this paper and in a preliminary account (18), we report on the quantitative labeling of PSI and PSII in thylakoid membranes from cells with different photosystem compositions, and provide evidence that photosystems are associated in clusters and that the PSII cluster size depends on the light growth conditions.

METHODS

Cell Culture. Cultures of *P. cruentum* (ATCC 50161) were grown at 18°C with 5% CO_2/95% air (19). Continuous light at ≈15 $\mu E \cdot m^{-2} \cdot s^{-1}$ was provided by daylight fluorescent lamps with a red filter (660-nm transmission maximum) for red light (RL) cells or a green filter (530-nm transmission maximum) for green light (GL) cells (17). Cultures were harvested in the late exponential phase of growth at densities between 4 and 6×10^6 cells per ml.

Thylakoid Isolation. Cell harvest and subsequent procedures were carried out under normal room light at 0°C–4°C. For PBsome-containing thylakoids, cells were harvested (5000 × *g*; 10 min), rinsed in 0.5 M potassium phosphate buffer (pH 7.0), suspended in SPC medium (0.3 M sucrose/0.5 M potassium phosphate/0.3 M potassium citrate, pH 7.0) (20), and broken in a French pressure cell (7000 psi; 1 psi = 6.9 kPa). The broken cell mixture was layered on a two-step gradient of sucrose (1.0 M and 1.3 M) in 0.5 M phosphate/0.3 M citrate, pH 7.0. After centrifugation for 30 min in a Beckman Microfuge 12, the PBsome-containing thylakoids were collected from the 1.0–1.3 M sucrose interface, applied directly to electron microscope grids, fixed for 1 min in 1% glutaraldehyde, rinsed in water, negatively stained with 1% uranyl acetate, and photographed at a magnification of ×21,000 in a Philips electron microscope.

For isolation of thylakoids for immunolabeling, cells were pelleted, rinsed briefly in deionized water, suspended in 25 mM Hepes·KOH (pH 7.5) and broken in a French press (3000 psi). The mixture was placed on a step gradient of sucrose (0.5, 1.0, 1.3, 2.0 M in 25 mM Hepes·KOH, pH 7.5) and, after 45 min at 35,000 rpm (SW40 Beckman rotor), thylakoids were collected from the 1.0–1.3 M sucrose region. They were diluted in 25 mM Hepes·KOH/10 mM EDTA, pH 7.5, and pelleted for 5 min in a Microfuge. Such thylakoids, largely free of phycobiliproteins, were gently resuspended and applied to electron microscope grids.

Antibody–Au Preparation. Production of antisera to PSI and PSII polypeptides and their affinity purification was as described by Mustardy *et al.* (13). For direct labeling, the affinity-purified IgG antibodies were individually conjugated to colloidal Au from Janssen Life Sciences (Piscataway, NJ) essentially according to the procedure described by the supplier (AuroProbe EM). The PSI antibody was conjugated to 10-nm Au, and the PSII antibody was conjugated to 15-nm Au. The conjugated antisera were stored at 10°C and used within a few days since reactivity declined with extended storage. For indirect labeling experiments, thylakoids were incubated with the same antibodies unattached to gold. Subsequent incubation with protein A–Au (10 nm) (Ted Pella, Redding, CA) served to label the bound antibody–antigen complexes. IgG from nonimmunized rabbits was used as a control.

Thylakoid Labeling. The thylakoid labeling procedure was carried out on Formvar/carbon-coated nickel electron microscope grids treated for 15 sec by "glow-discharge" to enhance thylakoid adhesion. Grids were kept in a Parafilm-lined chamber over crushed ice. A drop of gradient-purified thylakoids suspended in buffered sucrose was placed on each grid and removed after 2 min by touching a piece of filter paper at a right angle to the grid. Thylakoids adhering to the grid surface were rinsed (three changes, 10 min each with 1 M NaBr/20 mM NaCl/5 mM $MgCl_2$/50 mM Tris·HCl, pH 7.8) to remove extrinsic proteins. This was followed by rinsing in buffered saline solution and fixing in 1% glutaraldehyde/0.1 M sodium phosphate buffer, pH 7.0, for 1 min. Subsequent treatment was at room temperature and included three rinses with deionized water, two rinses within 1 min of 80% acetone, and two rinses with deionized water. Both sides of the grid were then treated for 20 min with 0.2% nonfat milk (Carnation) in buffered saline. The IgG–Au was suspended in 1% bovine serum albumin/20 mM Tris-buffered saline/20% (vol/vol) glycerol/20 mM NaN_3, pH 9.0. Each grid was placed on a drop (25–30 μl) of Au–IgG antibody solution for 20 h. The sample was kept on Parafilm in a covered Petri plate surrounded by wet filter paper. The covered Petri plate rested on an inverted Petri dish on a magnetic stirrer turning slowly to provide gentle agitation of the nickel grid. The overnight incubation was followed by gentle rinsing of the grid with a stream of deionized water. The grid was finally stained and photographed as described above.

For indirect labeling, thylakoids were treated as for direct labeling, except that they were incubated 20 h with the specific primary antibodies, rinsed, blocked, and labeled with protein A–Au (10 nm) for 30 min or 2 h (with the same results).

Quantitation. Numbers of PBsomes and Au particles per thylakoid area were counted on photographic prints of known magnification. Clumping of Au particles was minimal (<10%). Care was taken to exclude areas of thylakoid membrane overlap or folding. The areas were determined by the cut-and-weigh technique and the density of labeling was calculated as Au particles per μm^2 membrane area. Au particles adhering to the support film (or possibly to submicroscopic membrane fragments) were considered background, and their numbers were subtracted from those over the membranes.

RESULTS

PBsome/Photosystem Density. Photosynthetic membranes from *P. cruentum* with distinctly different PSI/PSII stoichiometries were used in these studies. They were isolated from cultures grown for many generations under RL (primarily absorbed by PSI) or GL (primarily absorbed by PBsomes). In cultures grown under RL, the PSII content was much higher and PSI content was substantially lower than in GL (17), whereas the PSI/PSII stoichiometry was not modified by light intensity (19).

PBsomes largely cover the surface of thylakoid membranes (Fig. 1 *A* and *B*) isolated in a medium that preserves both the capacity for excitation energy transfer from PBsomes to the photosystems and the ability to evolve oxygen at rates comparable to whole cells (20). The PBsome density in GL thylakoids is only slightly less (≈13%) than in RL thylakoids. The size (50 × 33 nm) and shape of PBsomes in GL and RL cells are the same whether attached to the membranes or when isolated on a sucrose gradient (Table 1). Cells grown in white light of comparable photon flux density contained PBsomes of the same size and density on the membranes (≈420 PBsomes per μm^2; data not shown) as those of GL and RL cells. We note that PBsomes do not occur in parallel rows in these thylakoid preparations. In fact, extended arrays of regular PBsome rows are rarely seen in isolated membranes, although they may be observed in chloroplast sections (21) of cells in which the density of membranes and PBsomes is high. Parallel PBsome arrays are likely a consequence of interdigitation resulting from close packing of thylakoid membranes rather than of any functional significance.

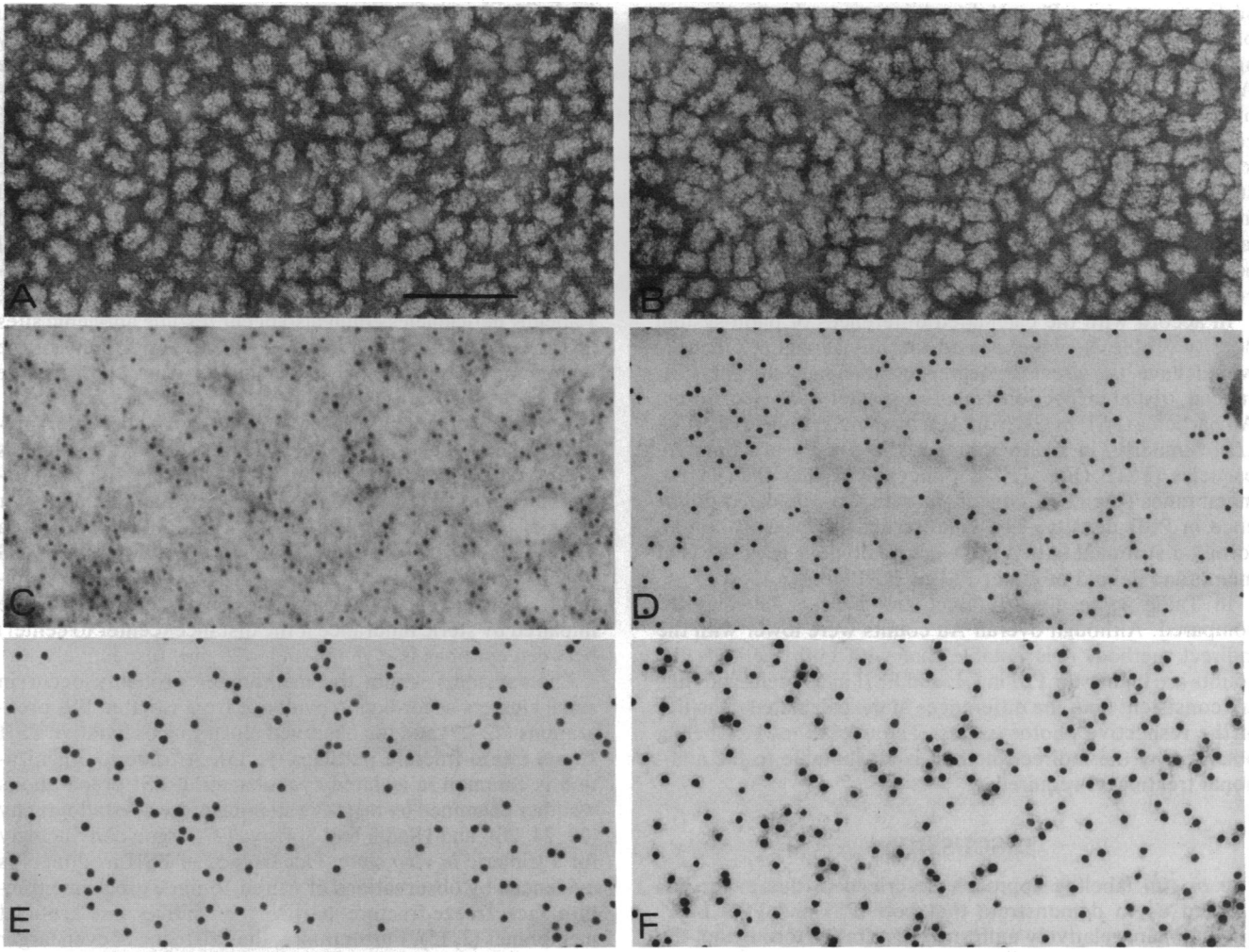

FIG. 1. Photosynthetic membranes from *P. cruentum* stained with uranyl acetate. PBsomes cover the membrane surface when isolated in 0.3 M sucrose/0.5 M phosphate/0.3 M citrate, pH 7.0 (*A* and *B*). Membranes stripped of extrinsic proteins and immunolabeled with 10-nm Au conjugates of anti-PSI (*C* and *D*) or 15-nm Au conjugates of anti-PSII (*E* and *F*). (*A*, *C*, and *E*) Membranes from GL-grown cells. (*B*, *D*, and *F*) Membranes from RL-grown cells. (Bar = 200 nm.) (×72,000.)

If the photosystems are distributed throughout the thylakoid membrane, then the number of PSI and PSII centers per unit area can be calculated (Table 2) from the number of PSI (P_{700}) and PSII (Q_A) per PBsome estimated from spectral determinations (17). In thylakoids of GL cells, we predict a density of ≈2520 PSI and ≈630 PSII per μm^2, with ≈1580 PSI and ≈1890 PSII per μm^2 in RL cells. The combined photosystem density (PSI and PSII) per μm^2 is comparable to estimates in green plants (2). The size of PBsomes is much larger than the sizes of PSI and PSII cores. Monomer sizes reported for PSI and PSII cores range from 65 to 100 nm^2 (2, 22–25) and appear to vary with the species and the techniques used for size estimation. We assume that the reaction centers of *Porphyridium*, as those of cyanobacteria, are like the reaction center cores of green plants. If each photosystem occupies a minimum surface area of 100 nm^2 then the thylakoid membrane area occupied by PSI and PSII together is ≈33% of the total. It is likely that most of the photosystems are completely overlaid by the PBsomes and it is expected that the PSII centers are located directly under the PBsome centers (21).

Table 1. PBsome density on thylakoids of *P. cruentum* grown under GL and RL of comparable irradiance

	PBsomes per μm^2	
	GL	RL
Experiment 1	393 ± 43	451 ± 25
Experiment 2	394 ± 40	451 ± 56

	PBsome dimensions, nm			
	Length	Width	Length	Width
PBsome attached	50 ± 4	33 ± 2	50 ± 5	33 ± 3
PBsome isolated	53 ± 4	33 ± 3	49 ± 5	34 ± 4

Continuous light at 15 $\mu E \cdot m^{-2} \cdot s^{-1}$ was provided. Data are means ± SD from 10 or more thylakoid areas.

PSI and PSII Distribution. In contrast to green plants, both PSI and PSII are distributed throughout the thylakoid membranes of GL and RL cells as indicated by the location of colloidal Au particles (Fig. 1 *C–F*). Maximal labeling of the photosystems required the removal of PBsomes and other

Table 2. Predicted densities of PSI and PSII per thylakoid area in *P. cruentum*

	Photosystems per PBsome*		Photosystem density per $\mu m^{2\dagger}$	
	GL	RL	GL	RL
PSI	6.4	3.5	2520	1580
PSII	1.6	4.2	630	1890

*From Table IV of Cunningham *et al.* (17).
†PBsomes per μm^2 (from Table 1) times photosystem per PBsome.

surface proteins. Phycobiliprotein removal was accomplished by rinsing in 25 mM Hepes·KOH, and the chaotropic agent NaBr (1 M) was required to remove the CF1 portion of ATP synthase. Thylakoids thus treated had chlorophyll fluorescence emission spectra (77 K, excitation at 440 nm) comparable to those in cells (data not shown). Partial delipidation after fixation of thylakoids was also required, presumably to remove chlorophyll and carotenoids, thus exposing antigenic regions of the photosystem polypeptides. The labeling density could not be increased by longer periods of acetone extraction (5 min) or by increasing the Au–antibody concentration or reaction time (up to 48 h).

In accord with the calculated differences of photosystem density (Table 2), we expected that thylakoids of GL cells would have the greatest degree of labeling with anti-PSI. Indeed, visual inspection reveals a greater density of 10-nm Au particles (PSI) in GL (Fig. 1*C*) than in RL thylakoids (Fig. 1*D*). Similarly, in RL membranes the density of 15-nm Au particles (PSII) (Fig. 1*F*) is noticeably higher than in GL membranes (Fig. 1*E*), consonant with the calculated difference in PSII density. The gold particles appear to be uniformly distributed in that there are no obvious large areas of membrane devoid of either PSI or PSII labels.

In Table 3, results of direct and indirect labeling are compared. Although overall Au counts were lower with the indirect method, it is notable that with both methods the counts are higher for PSI in GL and PSII in RL cells and thus are consistent with the differences in the calculated densities of the respective photosystems. The overall lower labeling obtained by the indirect method is attributable to the additional treatments required.

DISCUSSION

The *in situ* labeling approach described in this paper has allowed us to demonstrate that both PSI and PSII in *P. cruentum* are relatively uniformly distributed throughout the thylakoid membrane (Fig. 1 *C–F*), in contrast to the segregation of the photosystems that occurs in green plants. In evaluating the number of photosystems labeled (Table 4), we found by the direct labeling method that 25% of the PSI of both GL- and RL-grown cells are marked by a 10-nm Au particle. In GL thylakoids, 33% of the PSII are marked by 15-nm Au particles, but in RL thylakoids only 17% are marked. Having refined our conditions until maximal Au–antibody labeling was attained we must consider why <100% of the photosystems are labeled. Some reduction of labeling may be a consequence of the noncovalent binding of the IgG–Au conjugates, if during the overnight labeling period some IgG molecules dissociate from the Au conjugate and react with antigenic sites. However, this would occur in all cases and thus would not account for the observed differences of PSII labeling in membranes of GL and RL cells. Labeling deficiencies could also occur if some antigenic sites are not exposed; however, because of the uniformity of the membrane treatments this also is unlikely to account for the differences for PSII labeling in RL vs. GL.

Table 3. Au labels for PSI and PSII per thylakoid area in *P. cruentum*

	Au labels per μm^2	
	GL	RL
Direct antibody labeling*		
PSI antibody with 10-nm Au		
Exp. 1	608 ± 90	465 ± 39
Exp. 2	660 ± 63	313 ± 67
Exp. 3	610 ± 60	—
Mean	626 ± 29	389 ± 107
PSII antibody with 15-nm Au		
Exp. 1	233 ± 35	315 ± 24
Exp. 2	184 ± 30	287 ± 50
Exp. 3	—	376 ± 30
Mean	208 ± 35	326 ± 46
Indirect labeling: Protein A–10-nm Au†		
PSI antibody		
Exp. 1	150 ± 27	139 ± 17
Exp. 2	202 ± 27	132 ± 9
Mean	176 ± 37	135 ± 5
PSII antibody		
Exp. 1	167 ± 19	170 ± 20
Exp. 2	113 ± 13	187 ± 44
Mean	140 ± 38	178 ± 12

*Data are means ± SD from 8–12 thylakoid areas.
†Data are means ± SD from 5–10 thylakoid areas.

Spatial distances, in the nanometer range, between individual photosystems as well as the sizes of the Au conjugates used as labels are critical factors. The sizes of the Au–antibody complexes are somewhat larger than the monomer sizes of PSI and PSII. Since the Au–anti-PSI complex has a combined diameter of 15 nm (10-nm Au plus a measured IgG "shell" width of 5 nm), while the Au–anti-PSII has a combined diameter of 20 nm, labeling of PSI and PSII will be impaired by steric hindrance if the distance (center to center) between epitopes is <15 nm and <20 nm, respectively.

Photosystems within the membranes probably occur in small clusters according to evidence from isolated PSI preparations (22–27) and the observed clustering of putative PSII 10-nm freeze-fracture particles (9, 15). A trimeric organization is common in isolated cyanobacterial PSI preparations whether examined by negative staining or by crystallography (22, 24, 26), and Hladik and Sofrova (27) argue convincingly for a trimeric *in vivo* state. Occurrence of PSII as dimers is evidenced by observations of paired 10-nm exoplasmic fracture face freeze-fracture particles in native and artificial membranes (2, 15). Furthermore, the existence of even larger PSII clusters is probable, since in *Porphyridium* four or five PSII centers may be functionally associated with one PBsome (7).

Exploratory experiments to assess spatial hindrance have been carried out. In one set of experiments, thylakoids were simultaneously labeled with anti-PSI and anti-PSII. In such experiments (data not shown), we found that the total Au density (10- and 15-nm Au) was lower than when thylakoids were labeled separately. In another set of experiments, we conjugated 5-nm Au to anti-PSII and found that the label density was greater (GL, 265 Au per μm^2; RL, 540 Au per μm^2) than when we used 15-nm Au (Table 3). Both results indicate that some of the photosystems are closer to one another than the sizes of the labels. In view of these results and of separate evidence for photosystem clustering, we believe that in interpreting our labeling data it is not reasonable to assume that each photosystem core is individually marked. Rather, with PSI trimer clusters, each cluster would be marked by one Au conjugate particle (10-nm Au; Table 4), with an actual labeling efficiency of 75% rather than 25%. Also, if every PSII dimer is marked by one Au conjugate

Table 4. Percentage of PSI and PSII sites labeled in *P. cruentum*

	GL	RL
PSI		
Direct labeling (10-nm Au)	25%	25%
Indirect labeling (10-nm Au)	7%	8%
PSII		
Direct labeling (15-nm Au)	33%	17%
Direct labeling (5-nm Au)	42%	29%
Indirect labeling (10-nm Au)	22%	9%

particle (15-nm Au; Table 4) then the labeling efficiency is 66% in GL and 34% in RL (vs. 33% in GL and 17% in RL for the monomers of PSII). We suggest that there is a different clustering of PSII under the two light-growth conditions and that in RL cells the PSII clusters are about twice as large as in GL cells. Thus, in GL cells we expect a preponderance of PSII dimers, and in RL cells we expect a preponderance of tetramers. Differential clustering during acclimation to different wavelength conditions may allow *Porphyridium* to enhance cooperativity in energy utilization and thus increase photosynthetic yield.

A dilemma arises relating to the number of PSII sites labeled versus the expected correspondence (≈1:1) of PSII clusters and PBsome number per membrane area, since it is generally assumed that all PSII complexes are connected to PBsomes. Our data show that the total PSII label density is lower than the PBsome density. In RL, the number of PSII labels is ≈72% of the known PBsome number (330 Au labels per 450 PBsomes per μm^2) but only ≈53% in GL-grown cells (210 Au labels per 390 PBsomes per μm^2). If there is an overall inefficiency (≈28%) in labeling of thylakoids due to the limitations of the technique as mentioned above, in GL cells there might be ≈20% of PBsomes without PSII. This leads us to question the general expectation of a constant PSII–PBsome association. Although direct evidence exists only for a PSII–PBsome association (10), it is important to keep in mind that the possibility remains that some PBsomes may interact directly with PSI. In fact, in analyzing energy distribution correlated with state I and II transitions, Malkin *et al.* (28) favor the possibility that under certain conditions (in state II with light II) there is a direct interaction of PBsomes with PSI. From our experiments with the GL cells (grown in light II) it is plausible to assume that some PBsomes are not connected with PSII and may instead be connected to PSI.

The immunolabeling technique described here now makes it possible to begin assessing thylakoid topography at a resolution in the nanometer range. Further enhancement of resolution, to ≈5 nm, should be feasible by reducing the size of the Au–antibody complex. Such resolution can provide a bridge between the detailed structures of individual photosystems derived by crystallography and the gross membrane structural information obtained from electron microscopy of sectioned membranes. This technique also has potential for quantitative assessment of many intrinsic proteins in membranes generally.

We appreciate Mr. Shi Tan's help and skill in preparing membranes. The work was supported in part by Grant DE-FG05-90ER20007 from the U.S. Department of Energy and in part by the Maryland Agricultural Experiment Station.

1. Simpson, D. & von Wettstein, D. (1989) *Carlsberg Res. Commun.* **54**, 55–65.
2. Staehelin, L. A. (1986) in *Encylopedia of Plant Physiology New Series: Photosynthetic Membranes and Light Harvesting Systems*, eds. Staehelin, L. A. & Arntzen, C. J. (Springer, Berlin), Vol. 19, pp. 1–84.
3. Lavergne, J. & Joliot, P. (1991) *Trends Biochem. Sci.* **16**, 129–134.
4. Ort, D. R. (1986) in *Encylopedia of Plant Physiology New Series: Photosynthetic Membranes and Light Harvesting Systems*, eds. Staehelin, L. A. & Arntzen, C. J. (Springer, Berlin), Vol. 19, pp. 143–196.
5. Glazer, A. N. & Melis, A. (1987) *Annu. Rev. Plant Physiol.* **38**, 11–45.
6. Stevens, C. L. R. & Myers, J. (1976) *J. Phycol.* **12**, 99–105.
7. Ley, A. (1984) *Plant Physiol.* **74**, 451–454.
8. Lefort-Tran, M., Cohen-Bazire, G. & Pouphile, M. (1973) *J. Ultrastruct. Res.* **44**, 199–209.
9. Giddings, T. H., Wasmann, C. & Staehelin, L. A. (1983) *Plant Physiol.* **71**, 409–419.
10. Gantt, E., Clement-Metral, J. D. & Chereskin, B. M. (1988) *Methods Enzymol.* **167**, 286–290.
11. Allred, D. R. & Staehelin, L. A. (1985) *Plant Physiol.* **78**, 199–202.
12. McKay, R. M. L. & Gibbs, S. L. (1990) *Planta* **180**, 249–256.
13. Mustardy, L., Cunningham, F. X., Jr., & Gantt, E. (1990) *Plant Physiol.* **94**, 334–340.
14. Cunningham, F. X., Jr., Mustardy, L. & Gantt, E. (1991) *Plant Cell Physiol.* **32**, 419–426.
15. Moerschel, E. & Schatz, G. (1987) *Planta* **172**, 145–154.
16. Hinshaw, J. E. & Miller, K. R. (1989) *J. Cell Biol.* **109**, 1725–1731.
17. Cunningham, F. X., Jr., Dennenberg, R. J., Jursinic, P. & Gantt, E. (1990) *Plant Physiol.* **93**, 888–895.
18. Gantt, E., Mustardy, L. & Cunningham, F. X., Jr. (1991) *Plant Physiol.*, Suppl. **96**, 15 (abstr.).
19. Cunningham, F. X., Jr., Dennenberg, R. J., Mustardy, L., Jursinic, P. & Gantt, E. (1989) *Plant Physiol.* **91**, 1179–1187.
20. Dilworth, M. F. & Gantt, E. (1981) *Plant Physiol.* **67**, 608–612.
21. Gantt, E. (1986) in *Encylopedia of Plant Physiology New Series: Photosynthetic Membranes and Light Harvesting Systems*, eds. Staehelin, L. A. & Arntzen, C. J. (Springer, Berlin), Vol. 19, pp. 260–268.
22. Almog, O., Shoham, G., Michaeli, D. & Nechushtai, R. (1991) *Proc. Natl. Acad. Sci. USA* **88**, 5312–5316.
23. Boekema, E. J., Wynn, R. M. & Malkin, R. (1990) *Biochim. Biophys. Acta* **1017**, 49–56.
24. Irrgang, K.-D., Boekema, E. J., Vater, J. & Renger, G. (1988) *Eur. J. Biochem.* **178**, 209–217.
25. Roegner, M., Muehlenhoff, U., Boekema, E. J. & Witt, H. T. (1990) *Biochim. Biophys. Acta* **1015**, 415–424.
26. Ford, R. C., Hefti, A. & Engel, A. (1990) *EMBO J.* **9**, 3067–3075.
27. Hladik, J. & Sofrova, D. (1991) *Photosynth. Res.* **29**, 171–175.
28. Malkin, S., Herbert, S. K. & Fork, D. C. (1990) *Biochim. Biophys. Acta* **1016**, 177–189.